BBA - Molecular Basis of Disease 1863 (2017) 2964–2972

Contents lists available at ScienceDirect

BBA - Molecular Basis of Disease

journal homepage: www.elsevier.com/locate/bbadis

An abnormal TRPV4-related cytosolic Ca^{2+} rise in response to uniaxial stretch in induced pluripotent stem cells-derived cardiomyocytes from dilated cardiomyopathy patients

Jun Lu[a,b], Yee-Ki Lee[c,d,e], Xinru Ran[c,d,e], Wing-Hon Lai[c,d,e], Ronald A. Li[g,h], Wendy Keung[h], Kennis Tse[h], Hung-Fat Tse[c,d,e,f,*], Xiaoqiang Yao[a,b,**]

[a] School of Biomedical Sciences and Li Ka Shing Institute of Health Science, The Chinese University of Hong Kong, Hong Kong, China
[b] Shenzhen Research Institute, The Chinese University of Hong Kong, Shenzhen, China
[c] Cardiology Division, Department of Medicine, The University of Hong Kong, Hong Kong, China
[d] Hong Kong-Guangdong Joint Laboratory on Stem Cell and Regenerative Medicine, The University of Hong Kong, Hong Kong, China
[e] Guangzhou Institutes of Biomedicine and Health, China
[f] Shenzhen Institutes of Research and Innovation, The University of Hong Kong, Hong Kong, China
[g] Ming Wai Lau Centre for Reparative Medicine, Karolinska Institutet, Sweden
[h] Dr. Li Dak-Sum Centre, The University of Hong Kong – Karolinska Institutet Collaboration in Regenerative Medicine, Hong Kong, China

ARTICLE INFO

Keywords:
TRPV4 channel
Dilated cardiomyopathy
Cell stretch
Calcium signaling
Human induced pluripotent stem cells

ABSTRACT

Dilated cardiomyopathy (DCM) is cardiac disease characterized by increased left ventricular chamber volume and decreased systolic function. DCM patient-specific human induced-pluripotent stem cells-derived cardiomyocytes (DCM-hiPSC-CMs) were generated. We found that uniaxial stretch elicited a cytosolic $[Ca^{2+}]_i$ rise in hiPSC-CMs. Compared to control-hiPSC-CMs, DCM-hiPSC-CMs displayed a greater magnitude of $[Ca^{2+}]_i$ responses to the cell stretch of 10–15% elongation in length. This stretch-induced $[Ca^{2+}]_i$ rise was abolished by removal of extracellular Ca^{2+} and markedly attenuated by TRPV4 inhibitors HC-067047 and RN-1734. Application of nifedipine and tranilast also reduced the $[Ca^{2+}]_i$ response but to a lesser degree. Moreover, the augmented $[Ca^{2+}]_i$ was decreased by cytochalasin D treatment. Taken together, our study for the first time demonstrated an abnormal TRPV4-related mechanosensitive Ca^{2+} signaling in DCM-hiPSC-CMs.

1. Introduction

Dilated cardiomyopathy (DCM) is a common cardiomyopathy characterized by ventricular chamber enlargement and impaired systolic function, leading to progressive heart failure and sudden cardiac death [1]. The genetic basis of DCM is partially known, with 30% of cases harboring mutations in genes coding for sarcomere, z-disc, cytoskeleton, mitochondrial and nuclear lamina [2]. Dysregulation of mechanical signaling is one of the contributing factors for DCM [3]. Excessive mechanical loads may result in maladaptive remodeling of heart, leading to cardiomyopathies including DCM [3,4]. DCM cardiomyocytes also display abnormal Ca^{2+} handling. In several animal models of DCM, there is an increase in amplitude and duration of Ca^{2+} transients in cardiomyocytes [5–8]. Mutation of the proteins that affect Ca^{2+} handling is associated with DCM [6,9–11].

Mechanosensitive ion channels are activated in response to mechanical stimuli [12]. The activity of these channels induces ion flux across the cells, resulting in changes of membrane potential and/or cytosolic $[Ca^{2+}]_i$ level, which then elicits cellular signaling cascades. Cardiac myocytes express multiple mechanosensitive Ca^{2+}-permeable transient receptor potential (TRP) channels, including TRPC1, -C3, -C5, -C6, -V1, -V2, -V4, and -P2 [13]. It is intriguing to postulate that dysregulation or dysfunction of some mechanosensitive TRP channels could alter Ca^{2+} signaling, contributing to DCM progression. Indeed, recent studies found an association between TRPV2 and DCM [14]. In DCM animal models as well as in DCM patients, TRPV2 was found to be abnormally accumulated in the sarcolemma [14]. Furthermore, blockade of sarcolemmal TRPV2 accumulation inhibited the progression of DCM [14].

We and others have successfully generated patient-specific hiPSC-CMs from DCM patients [10,11,15]. These iPSC-CMs from DCM patients recapitulate to some extent the pathogenic phenotypes of DCM, thus

* Correspondence to: H.-F. Tse, Division of Cardiology, Department of Medicine, The University of Hong Kong, Queen Mary Hospital, Pokfulam, Hong Kong, China.
** Correspondence to: X. Yao, School of Biomedical Sciences, The Chinese University of Hong Kong, Shatin, Hong Kong, China.
E-mail addresses: hftse@hku.hk (H.-F. Tse), yao2068@cuhk.edu.hk (X. Yao).

http://dx.doi.org/10.1016/j.bbadis.2017.07.021
Received 13 March 2017; Received in revised form 15 June 2017; Accepted 24 July 2017
Available online 25 July 2017

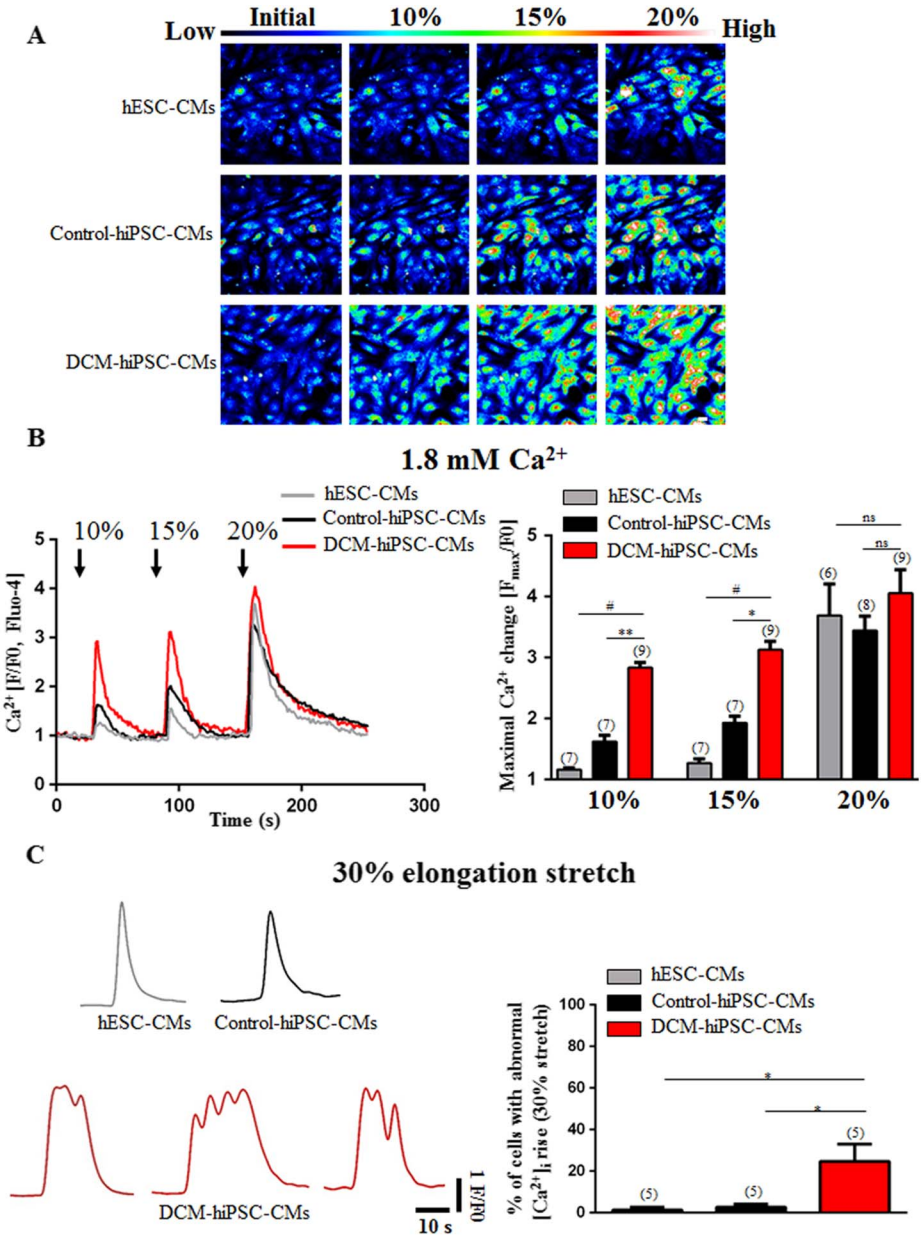

Fig. 1. Uniaxial cell stretch elicits a $[Ca^{2+}]_i$ rise in hESC-CMs, control-hiPSC-CMs and DCM-hiPSC-CMs. (A) Representative pseudo-color images showed the changes in the fluo-4 fluorescence signal of hESC-CMs, control-hiPSC-CMs and DCM-hiPSC-CMs before and after uniaxial stretch equivalent to 10%, 15% and 20% elongation in Tyrode's solution containing 1.8 mM Ca^{2+}. (B) Representative time course traces of $[Ca^{2+}]_i$ rise in response to different stretch elongation (left) and data summary of the peak florescence value after the stretch (right). (C) Representative traces of stretch-induced $[Ca^{2+}]_i$ rise in response to 30% uniaxial elongation (left) and data summary showing the percentages of DCM-hiPSC-CMs with abnormal Ca^{2+} transients under 30% stretch (right). Values in data summary are mean ± SEM (n = 5–9 experiments). $^{*}P < 0.05$, $^{**}P < 0.01$, $^{\#}P < 0.001$, ns = not significant.

may serve as a useful platform for exploring disease mechanisms. One of these DCM-hiPSC-CM lines carries a point mutation in desmin proteins (A285V-DES) [15]. Desmin (DES) is an intermediate filament protein that interacts with other proteins to maintain cytoskeletal organization, force transmission and mechano-chemical signaling within cardiomyocytes [16]. DES mutations are linked to DCM [17,18].

Previously, TRPV4 was reported to mediate stretch-induced Ca^{2+} influx in urothelial cells and oesophageal keratinocytes [19,20]. Recently, we also found an important functional role of TRPV4 in mediating stretch-induced cytosolic $[Ca^{2+}]_i$ rise in human embryonic stem cell-derived cardiomyocytes [21]. However, it is unclear whether TRPV4-mediated $[Ca^{2+}]_i$ response is altered in DCM cardiomyocytes. In the present study, we utilized the DCM-hiPSC-CMs generated from A285V-DES patients as the DCM model to investigate TRPV4 involvement in stretch-induced $[Ca^{2+}]_i$ response. Our results demonstrated that DCM-hiPSC-CMs had a greater $[Ca^{2+}]_i$ rise in response to mechanical stretch than that of control-hiPSC-CMs. This abnormal $[Ca^{2+}]_i$ response was mostly related to TRPV4 with some contribution from TRPV2 and L-type Ca^{2+} channels.

2. Material and methods

2.1. Generation of human induced pluripotent stem cells and cardiac differentiation

Detailed methods on hiPSC generation and characterization, and *in vitro* cardiac differentiation have been previously reported [15]. Skin biopsies were obtained under standard aseptic technique from a 43-year-old Caucasian man with dilated cardiomyopathy. Fibroblasts were reprogrammed to hiPSCs via retroviral transduction of Yamanaka transcription factors OCT-4, SOX2, KLF4 and c-MYC [22]. Cardiac differentiation of hiPSCs (IMR90, WiCell) clone and human ES cell line (HES2) were achieved via Wnt signaling [23]. Cardiac-spheres on days 30–40 were digested with 1 mg/ml collagenase type IV (Invitrogen) and 0.1 mg/ml DNase I (Sigma) at 37 °C for 30 min, followed by 0.05% trypsin (Invitrogen) at 37 °C for 5 min to derive single cardiomyocytes. After dispersal, the cells were seeded onto matrigel (BD Biosciences, Franklin Lakes, NJ)-coated silicone stretch chamber (ST-CH-04, B-Bridge International, Inc.) and were fed every other day with serum-free RPMI-B27 medium (Life Technologies). After 1–2 days, the cells

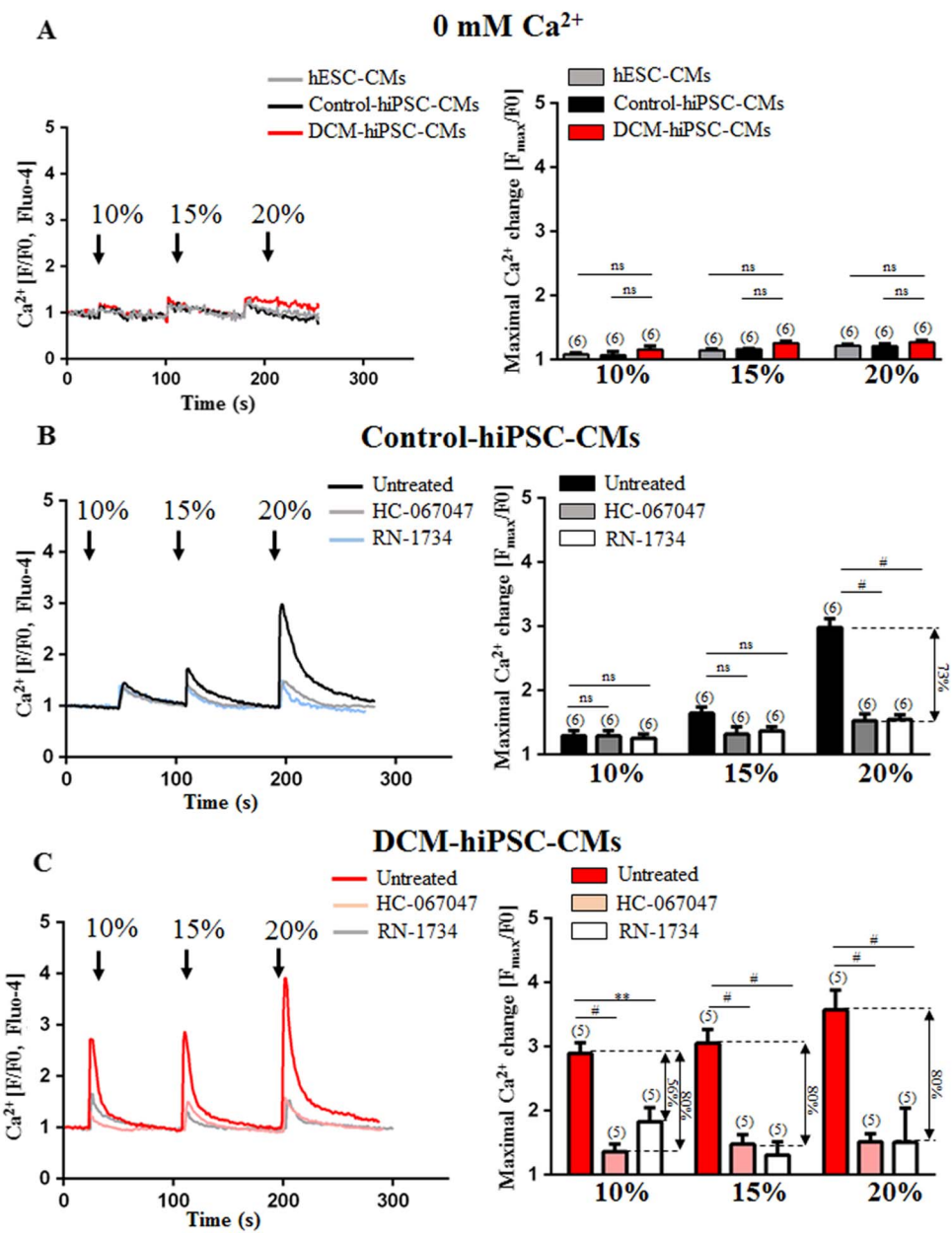

Fig. 2. TRPV4 channels are the major contributor mediating the stretch-induced Ca^{2+} influx. (A) Representative time course traces of $[Ca^{2+}]_i$ rise in response to different stretch elongation (left) and data summary of the peak florescence value after the stretch (right) in the absence of extracellular Ca^{2+}. (B and C) Representative time course traces of $[Ca^{2+}]_i$ rise in response to different stretch elongation (left) and data summary of the peak florescence value after the stretch (right) before and after 1 μM HC-067047 or 10 μM RN-1734 treatment in control-hiPSC-CMs (B) and DCM-hiPSC-CMs (C). The cells were stretched without inhibitors, followed by application of inhibitors and then another series of stretch. Values in data summary are mean ± SEM (n = 5–6 experiments). $^{**}P < 0.01$, $^{**}P < 0.01$, $^{\#}P < 0.001$, ns = not significant.

were ready for stretching experiments. α-actinin immunofluorescence staining was performed to confirm cardiac phenotype. Flow cytometry analysis performed on differentiated cardiomyocytes showed 90% of cells were c-TnT^+.

2.2. Mechanical stretch experiment

Uniaxial mechanical stretch was applied to hESC-CMs, control-hiPSC-CMs and DCM-hiPSC-CMs using STREX cell stretching system (ST-150; Strex, B-Bridge International, Inc.). The chamber was uniaxially stretched equivalent to 10%, 15%, 20% or 30% elongation of the initial length for 3 s and was returned to the initial unstretched state at room temperature. In the preliminary study, we also tested the stretch time duration of 1 s and found no difference in stretch-induced $[Ca^{2+}]_i$ rise between the stretch duration of 1 s and 3 s (Supplementary Fig. 1).

2.3. Reagents

Stock solutions of nifedipine (Sigma), HC-067047 (Sigma), RN-1734 (Santa Cruz Biotechnology, Inc.), Pyr3 (Sigma), tranilast (Sigma), SAR7334 (MedChem Express) and MS-PPOH (Santa Cruz Biotechnology, Inc.) were prepared in DMSO. The final concentration of DMSO was 0.1% in each experiment. 17-Octadecynoic acid (17-ODYA) (Cayman Chemical) and Cytochalasin D (Sigma) were dissolved in ethanol. Capsazepine (Sigma) was dissolved in methanol. Clemizole (TOCRIS) and amiloride (Sigma) was prepared in H_2O. T1E3 antibody and preimmune IgG were prepared as described elsewhere [24]. All other chemicals were purchased from Sigma.

2.4. Ca^{2+} imaging

hESC-CMs, control-iPSC-CMs or DCM-iPSC-CMs were loaded with fluo-4/AM (Invitrogen, 5 μM) and 0.02% Pluronic F-127 (Invitrogen) for 30 min in dark at 37 °C, which then were observed with a confocal microscope (Olympus FV1000). Fluo-4 was excited at 488-nm line and captured at wavelengths 505–530 nm. Two-dimensional images were obtained with the confocal microscope operating in the frame-scan (X–Y, 320 × 320 pixels). Changes in $[Ca^{2+}]_i$ were displayed as a ratio

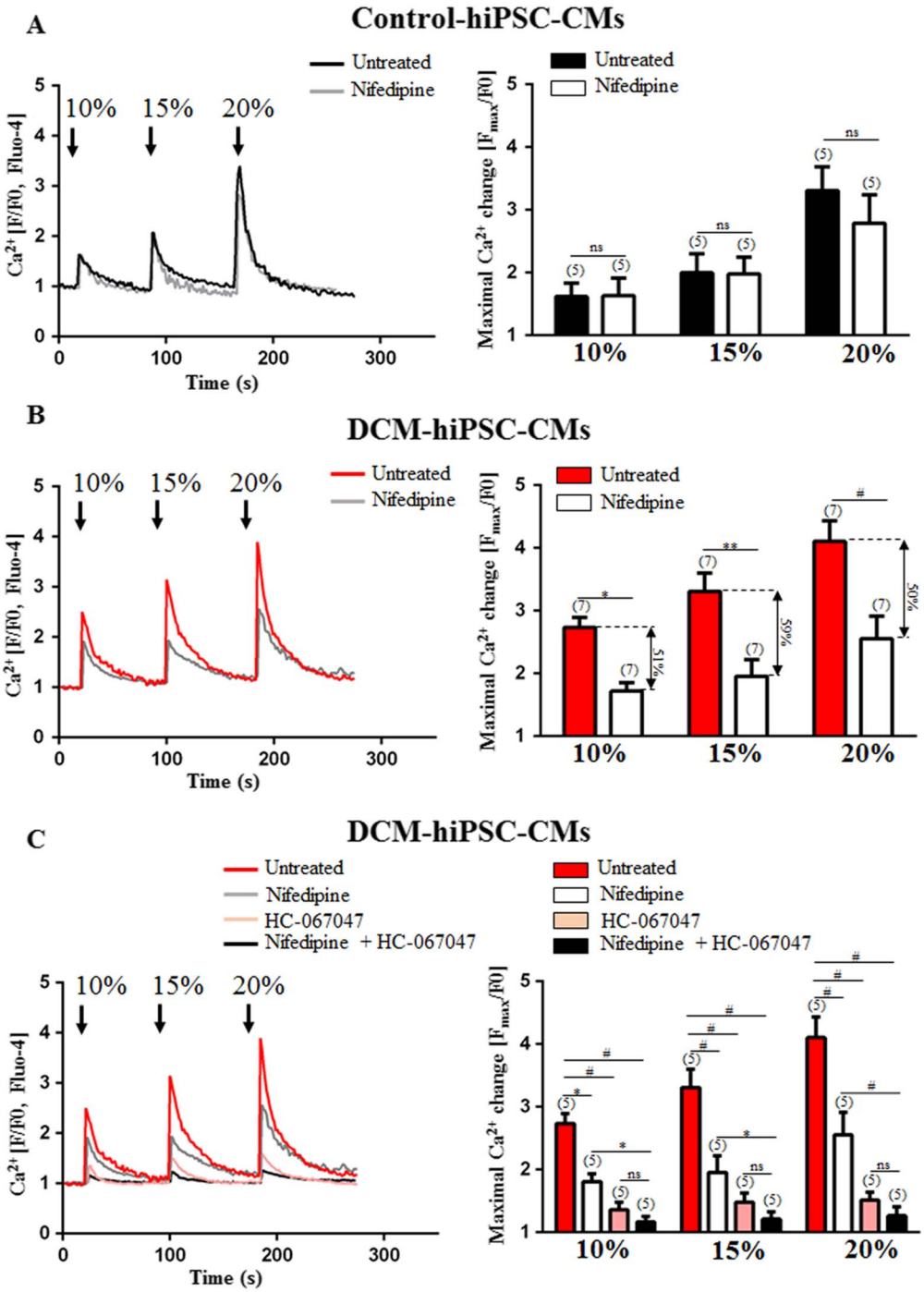

Fig. 3. L-type Ca^{2+} channels partially contribute to the stretch-induced Ca^{2+} influx in DCM-hiPSC-CMs. Shown are representative time course traces of $[Ca^{2+}]_i$ rise in response to different stretch elongation (left) and data summary of the peak florescence value after the stretch (right) before and after 10 μM nifedipine (A–C) or 1 μM HC-067047 (C) or combined application of 10 μM nifedipine + 1 μM HC-067047 (C) in control-hiPSC-CMs (A) and DCM-hiPSC-CMs (B and C). The cells were stretched without inhibitors, followed by application of inhibitors and then another series of stretch. Values in data summary are mean ± SEM (n = 5–7 experiments). $^{*}P < 0.05$, $^{**}P < 0.01$, $^{\#}P < 0.001$, ns = not significant.

of fluorescence relative to the basal intensity before the application of extracellular Ca^{2+} (F/F0). Ca^{2+} imaging experiments were performed in Tyrode's solution containing in mM: NaCl 140, KCl 5.4, $CaCl_2$ 1.8, $MgCl_2$ 1, glucose 10, HEPES 10, adjusted to pH 7.40 with NaOH. Some experiments were carried out in a Ca^{2+}-free Tyrode's solution, which contained in mM: NaCl 140, KCl 5.4, EGTA 1, $MgCl_2$ 1, glucose 10, HEPES 10, adjusted to pH 7.40 with NaOH.

2.5. Immunoblotting

For immunoblotting experiments, twenty micrograms of cardiomyocyte lysates were resolved on SDS/PAGE. Membrane was incubated with primary antibodies: anti-TRPV4 (1:1000, Alomone Labs), anti-TRPC1 (1:1000, Alomone Labs), anti-TRPC3 (1:1000, Alomone Labs), anti-TRPC5 (1:1000, Proteintech), anti-TRPC6 (1:1000, Alomone Labs), anti-TRPV1 (1:1000, Alomone Labs), anti-TRPV2 (1:1000, Alomone Labs), anti-TRPP2 (1:500, Santa Cruz Biotechnology Inc.) and β-actin (1:3000, Santa Cruz Biotechnology Inc.). Samples were detected with Amersham ECL Western Blotting Detection Reagent (GE Healthcare). For all immunoblotting experiments, the protein concentration was measured by using the DC™ protein assay (Bio-Rad).

2.6. Statistical analysis

The experimental results were expressed as means ± SEM. Independent experiments using different batches of differentiated cardiomyocytes were used as the repeats in statistical analysis. Statistical significance was evaluated by using Student's t-test, one-way analysis of

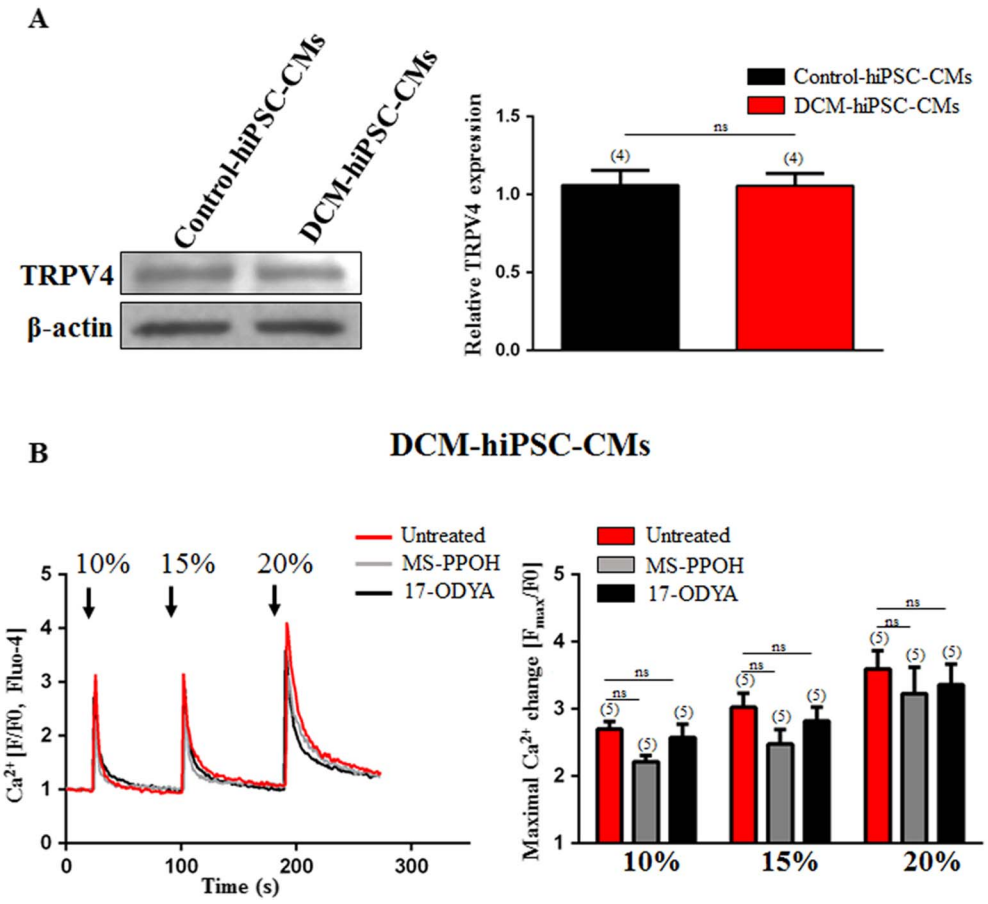

Fig. 4. TRPV4 protein expression and cytochrome P450 epoxygenases in control-hiPSC-CMs and DCM-hiPSC-CMs. (A) Representative immunoblot images (left) and data summary (right) of TRPV4 protein expression. β-actin was used as the loading control. (B) representative time course traces of $[Ca^{2+}]_i$ rise in response to different stretch elongation (left) and data summary of the peak florescence value after the stretch (right) before and after 30 μM MS-PPOH or 10 μM 17-ODYA treatment in DCM-hiPSC-CMs. The cells were stretched without inhibitors, followed by application of inhibitors and then another series of stretch. Values in data summary are mean ± SEM (n = 4–5 experiments), ns = not significant.

variance (ANOVA) or two-way analysis of variance (ANOVA) followed by Bonferroni post-tests using Prisms 6.0 software (GraphPad Software Inc., La Jolla, CA, USA). $P < 0.05$ was considered statistically significant.

3. Results

3.1. $[Ca^{2+}]_i$ rise in response to uniaxial cell stretch

hESC-CMs, control-hiPSC-CMs and DCM-hiPSC-CMs seeded onto matrigel-coated silicon stretch chambers were subjected to uniaxial stretch equivalent to 10%, 15%, 20% and 30% elongation of the initial length for 3 s and then returned to original position. Most cardiomyocytes exhibited a transient $[Ca^{2+}]_i$ rise in response to 10–20% stretch (Fig. 1A). Fig. 1B showed a typical time course of $[Ca^{2+}]_i$ rise in response to different degree of uniaxial stretch in representative cardiomyocytes. Compared with hESC-CMs and control-hiPSC-CMs, DCM-hiPSC-CMs displayed a greater magnitude of $[Ca^{2+}]_i$ response to the cell stretch of 10% elongation in length and 15% elongation in length (Fig. 1B). However, under 20% stretch, there was no apparent difference in $[Ca^{2+}]_i$ rise among the three cell types (Fig. 1B). In addition, under excessive stretch of 30%, ~25% of DCM-hiPSC-CMs displayed a more prolonged Ca^{2+} transient with small oscillation, which was not observed in control-hiPSC-CMs or hESC-CMs (Fig. 1C). These results showed that DCM-hiPSC-CMs had a greater $[Ca^{2+}]_i$ response to mechanical stretch.

3.2. TRPV4 channels are the major contributor in stretch-induced Ca^{2+} influx

Next we examined the role of extracellular Ca^{2+} entry in this $[Ca^{2+}]_i$ rise. In the absence of extracellular Ca^{2+}, uniaxial stretch was only able to induce a very small magnitude of $[Ca^{2+}]_i$ rise (Fig. 2A), suggesting that extracellular Ca^{2+} entry is a prerequisite for this stretch-induced $[Ca^{2+}]_i$ rise.

Next we determined the possible involvement of TRPV4 channels in the stretch-induced $[Ca^{2+}]_i$ rise. HC-067047 and RN-1734 are two highly selective inhibitors of TRPV4 [25]. In control-hiPSC-CMs, 1 μM HC-067047 and 10 μM RN-1734 had no obvious effect on the stretch-induced $[Ca^{2+}]_i$ rise in the stretch range of 10%–15%. The inhibitory effect of 1 μM HC-067047 and 10 μM RN-1734 on the $[Ca^{2+}]_i$ rise only became obvious when the stretch reached 20% (Fig. 2B). In contrast, in DCM-hiPSC-CMs, the peak magnitude of stretch-induced $[Ca^{2+}]_i$ rise was markedly inhibited by 1 μM HC-067047 or 10 μM RN-1734 in the all stretch range (10%, 15% and 20%) (Fig. 2C). Interestingly, 1 μM HC-067047 or 10 μM RN-1734 both reduced the abnormally high $[Ca^{2+}]_i$ response in DCM-hiPSC-CMs to a very low level, similar to that of control-hiPSC-CMs. The inhibition was about 80% in DCM-hiPSC-CMs (Fig. 2C). These results suggest that the abnormally high stretch-induced $[Ca^{2+}]_i$ response in DCM-hiPSC-CMs was largely associated with the activity of TRPV4 channels.

3.3. L-type Ca^{2+} channels also contribute to the stretch-induced Ca^{2+} influx

Nifedipine, a selective inhibitor of L-type Ca^{2+} channels, was used to test the involvement of L-type Ca^{2+} channels in the stretch-induced $[Ca^{2+}]_i$ rise. Interestingly, while nifedipine (10 μM) had no effect on the stretch-induced $[Ca^{2+}]_i$ rise in control-hiPSC-CMs (Fig. 3A), it significantly reduced the stretch-induced $[Ca^{2+}]_i$ rise in DCM-hiPSC-CMs (Fig. 3B). Therefore, the involvement of L-type Ca^{2+} channels in the stretch $[Ca^{2+}]_i$ response appears to be a unique property of DCM-hiPSC-CMs. Note that, compared to nifedipine, TRPV4 antagonists had substantially greater inhibition on the stretch-induced $[Ca^{2+}]_i$ rise in

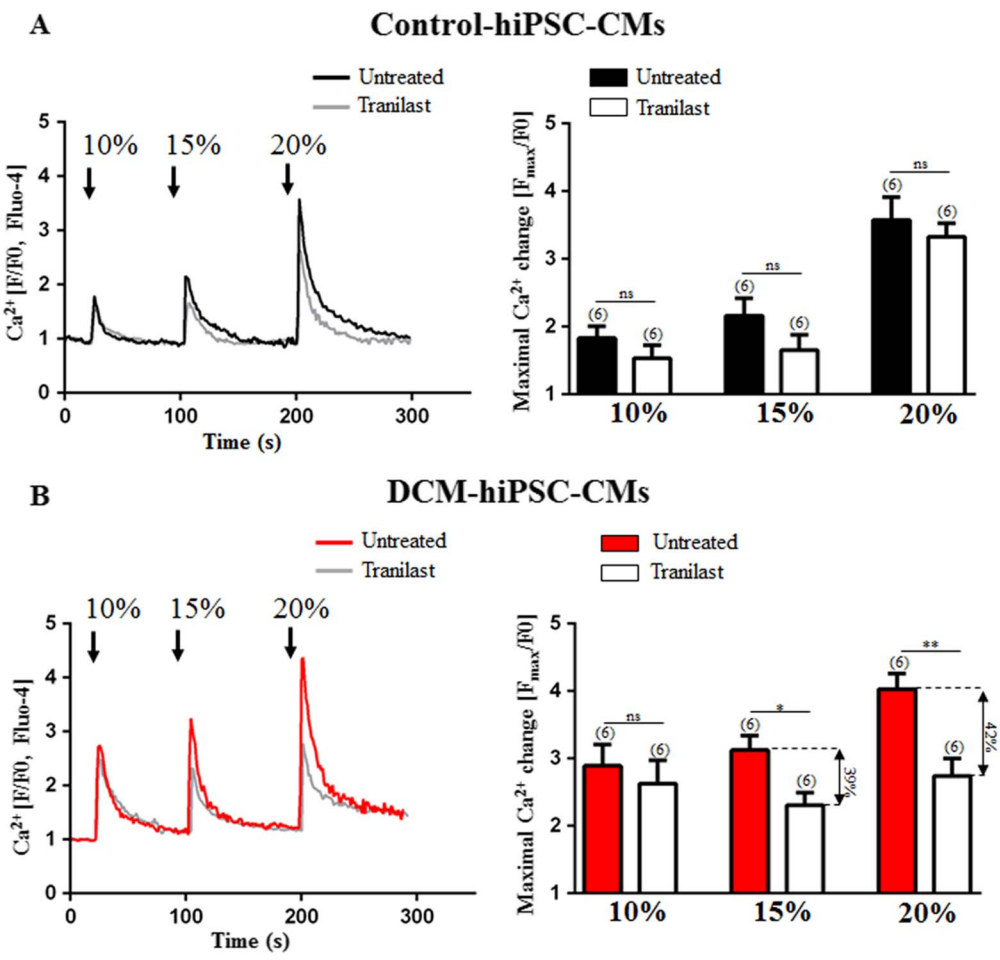

Fig. 5. TRPV2 channels partially contribute to the stretch-induced Ca^{2+} influx in DCM-hiPSC-CMs. Shown are representative time course traces of $[Ca^{2+}]_i$ rise in response to different stretch elongation (left) and data summary of the peak florescence value after the stretch (right) before and after 75 μM tranilast treatment in control-hiPSC-CMs (A) and DCM-hiPSC-CMs (B). The cells were stretched without inhibitors, followed by application of tranilast and then another series of stretch. Values in data summary are mean ± SEM (n = 6 experiments). $^{*}P < 0.05$, $^{**}P < 0.01$, ns = not significant.

DCM-hiPSC-CMs (80% inhibition for TRPV4 inhibitors *vs.* 50% inhibition for nifedipine at 20% cell stretch. Combined application of 10 μM nifedipine + 1 μM HC-067047 had more effect than nifedipine alone, but was similar to that of 1 μM HC-067047 alone (Fig. 3C).

3.4. TRPV4 expression and cytochrome P450 epoxygenases in control-hiPSC-CMs and DCM-hiPSC-CMs

Immunoblots were performed to compare the expression level of TRPV4 proteins between control-hiPSC-CMs and DCM-hiPSC-CMs. Fig. 4A showed that TRPV4 protein level was not significantly upregulated in DCM-hiPSC-CMs. Furthermore, the expression level of TRPV4 was not different among iPSC-CMs at different differentiation stages, adult mouse heart samples and neonatal rat cardiomyocytes (Supplementary Fig. 2).

It is well documented that hypotonicity-induced cell swelling can activate TRPV4 via cytochrome P450 epoxygenases and epoxyeicosatrienoic acids [26]. However, inhibition of cytochrome P450 epoxygenases by 30 μM MS-PPOH or 10 μM 17-ODYA failed to alter the stretch-induced $[Ca^{2+}]_i$ response in DCM-hiPSC-CMs (Fig. 4B).

3.5. Role of other mechanosensitive Ca^{2+}-permeable channels

Possible involvement of several other mechanosensitive Ca^{2+}-permeable channels, including TRPC1, -C3, -C5, -C6, -V1, -V2 and -P2, in the stretch response of hiPSC-CMs was also explored. Immunoblot results showed no difference in the protein expression of all these isoforms between control-hiPSC-CMs and DCM-hiPSC-CMs (Supplementary Fig. 3). Functional inhibition by selective pharmacological antagonists or blocking antibody, TRPC1 by 10 μg/ml T1E3 blocking antibody [24], TRPC3 by 10 μM Pyr3 [27], TRPC5 by 4 μM clemizole [28], TRPC6 by 100 nM SAR7334 [29], TRPV1 by 10 μM capsazepine [30] and TRPP2 by 100 μM amiloride [31], had no effect on the stretch-induced $[Ca^{2+}]_i$ rise in control-hiPSC-CMs and DCM-hiPSC-CMs (Supplementary Fig. 4). Interestingly, while inhibition of TRPV2 by 75 μM tranilast [32] did not alter the stretch-induced $[Ca^{2+}]_i$ in control-hiPSC-CMs, this treatment did reduce the stretch-induced $[Ca^{2+}]_i$ rise in DCM-hiPSC-CMs by ~40% at the cell stretch ranges of 15%–20% (Fig. 5). On the other hand, at 10% cell stretch 75 μM tranilast had no effect on the stretch-induced $[Ca^{2+}]_i$ rise in DCM-hiPSC-CMs (Fig. 5).

3.6. Actin cytoskeleton is involved in stretch-induced Ca^{2+} influx

It has been suggested that mechanical force may transmit through cytoskeleton to activate TRPV4 and TRPV2 [33,34] and that actin cytoskeleton could modulate stretch-mediated Ca^{2+} influx [34–36]. We used 10 μM cytochalasin D to disrupt actin polymerization [37]. In control-hiPSC-CMs, treatment with cytochalasin D for 30 min reduced the stretch-induced $[Ca^{2+}]_i$ rise only at 20% stretch but not in the stretch range of 10–15%. In contrast, in DCM-hiPSC-CMs, 10 μM cytochalasin D treatment reduced the stretch-induced $[Ca^{2+}]_i$ rise at both 15% and 20% stretching ranges. Compared to control-hiPSC-CMs, the effect of cytochalasin D was greater in DCM-hiPSC-CMs (Fig. 6A and B).

4. Discussion

In the present study, we utilized patient-specific iPSC-derived cardiomyocytes as DCM model to investigate the stretch-induced $[Ca^{2+}]_i$ change and obtained the following findings: a) Uniaxial stretch elicited

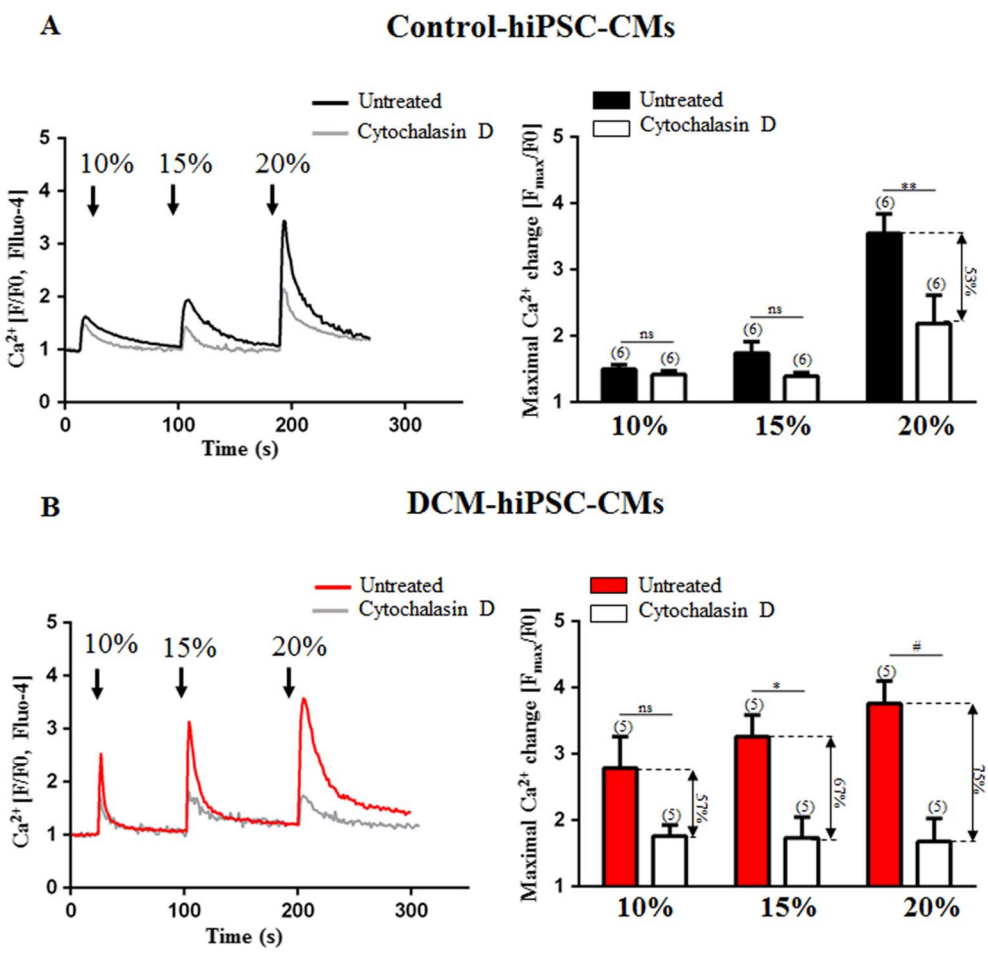

Fig. 6. Actin cytoskeleton is involved in stretch-induced Ca^{2+} influx. Shown are representative time course traces of $[Ca^{2+}]_i$ rise in response to different stretch elongation (left) and data summary of the peak florescence value after the stretch (right) before and after 10 μM cytochalasin D treatment in control-hiPSC-CMs (A) and DCM-hiPSC-CMs (B). The cells were stretched without inhibitors, followed by application of cytochalasin D and then another series of stretch. Values in data summary are mean ± SEM (n = 5–6 experiments). $^{*}P < 0.05$, $^{**}P < 0.01$, $^{\#}P < 0.001$, ns = not significant.

a $[Ca^{2+}]_i$ rise in hiPSC-CMs. The magnitude of $[Ca^{2+}]_i$ rise was positively correlated with the degree of cell stretch. b) Compared to control-hiPSC-CMs, DCM-hiPSC-CMs displayed a greater magnitude of $[Ca^{2+}]_i$ responses to cell stretch, especially in the range of low to moderate stretch (10–15%). c) This stretch-induced $[Ca^{2+}]_i$ rise was substantially reduced by TRPV4 inhibitors HC-067047 and RN-1734, suggesting that an important role of TRPV4. Nifedipine and tranilast also attenuated the $[Ca^{2+}]_i$ response but to a lesser degree, suggesting some participation of L-type Ca^{2+} channels and TRPV2 channels. d) Cytochalasin D treatment reduced the stretch-induced $[Ca^{2+}]_i$ response to a greater degree in DCM-hiPSC-CMs than in control-hiPSC-CMs. Taken together, our study for the first time demonstrated an abnormal TRPV4-mediated mechanosensitive Ca^{2+} signaling in DCM-hiPSC-CMs.

DCM is characterized by cardiac dilation and reduced systolic function [1]. DCM cardiomyocytes show abnormal Ca^{2+} handlings. In several animal models of DCM, there is an increase in the amplitude and duration of Ca^{2+} transients in cardiomyocytes [5–8]. DCM cardiomyocytes also display abnormal mechanical response [38]. Mutations in cytoskeleton desmin and nuclear lamins are known to cause the pathogenesis of DCM [17,39]. However, up to the present, there is still no report about an altered $[Ca^{2+}]_i$ response to mechanical stretch in DCM cardiomyocytes. In this study, we clearly demonstrated a much greater $[Ca^{2+}]_i$ response to unidirectional stretch in DCM-hiPSC-CMs than in control-hiPSC-CMs. It is previously documented that 10% cell elongation (stretch) is considered to be “physiological” while a cell elongation of 20% or more is considered to be pathological [40,41]. Interestingly, greater differences in the amplitude of stretch-induced $[Ca^{2+}]_i$ responses between control-hiPSC-CMs and DCM-hiPSC-CMs were found in the physiological stretching range of 10%, suggesting its physiological relevance. Furthermore, highly selective TRPV4 inhibitors HC-067047 and RN-1734 strongly inhibited the stretch-induced $[Ca^{2+}]_i$ response in DCM-hiPSC-CMs by up to 80% in all stretching ranges including the physiological stretching range of 10%, suggesting a major role of TRPV4. Moreover, under excessive mechanical stretch of 30%, the shape of stretch-induced $[Ca^{2+}]_i$ transient in DCM-hiPSC-CMs became grossly abnormally, appearing more prolonged with some small oscillations. Previous reports from others have proposed that an abnormally high Ca^{2+} level in cardiomyocytes may stimulate apoptosis, thereafter weaken the contractility of cardiac muscle and exacerbate DCM progression [5,42]. Our present study uncovered an abnormality in TRPV4-mediated $[Ca^{2+}]_i$ response in DCM cardiomyocytes. Cardiomyocytes *in vivo* are constantly subjected to cyclic contraction and relaxation/extension during cardiac cycle. It is highly likely that the abnormally high TRPV4-mediated $[Ca^{2+}]_i$ response to stretch cycle may induce apoptotic cell death, leading to the pathological progression of DCM.

Also note that TRPV4 may not be the only TRP channels involved in DCM. A recent study suggests that TRPV2 may also play a role in DCM progression [14]. Indeed, we also found that inhibition of TRPV2 by tranilast reduced the stretch-induced $[Ca^{2+}]_i$ response in DCM-hiPSC-CMs. However, the effect of TRPV2 inhibition on the stretch-induced $[Ca^{2+}]_i$ response was much smaller than that of TRPV4 inhibition at the cell stretch ranges of 15%–20% (Figs. 2 and 5). Furthermore, the effect of TRPV2 inhibition was absent in the physiological stretching range of 10% (Fig. 5). Together, our data suggest that Ca^{2+} entry through several TRPs, including TRPV4 and to a lesser degree TRPV2, may affect DCM disease progression.

We also found that nifedipine could partially inhibit the stretch-evoked $[Ca^{2+}]_i$ response in DCM-hiPSC-CMs but not in control-hiPSC-CMs (Fig. 2B–C), suggesting an involvement of L-type Ca^{2+} channels in

the stretch response in DCM-hiPSC-CMs. Because L-type Ca^{2+} channels cannot be directly activated by cell stretch [43–45], we postulate that the activation of L-type Ca^{2+} channels is a secondary response after TRPV4 and TRPV2 activation. It is likely that, in DCM-hiPSC-CMs, excessive activities of TRPV4 and TRPV2 under cell stretch result in membrane depolarization, which subsequently activates voltage-gated L-type Ca^{2+} channels. A similar scheme, which links TRPC6-mediated membrane depolarization to the activity of L-type Ca^{2+} channels was previously proposed in vascular smooth muscle [46]. Another point to note is that cardiomyocytes possess a well-characterized mechanism of Ca^{2+}-induced Ca^{2+} release [47], in which extracellular Ca^{2+} entry through plasma membrane channels serves to stimulate intracellular Ca^{2+} release from sarcoplasmic reticulum. Therefore, overall amount of $[Ca^{2+}]_i$ rise is attributed to both extracellular Ca^{2+} entry and intracellular Ca^{2+} release. It is likely that an abnormally high Ca^{2+} entry via TRPV4, TRPV2 and L-type Ca^{2+} channels would induce more Ca^{2+} release from sarcoplasmic reticulum, both of which contribute to the excessive $[Ca^{2+}]_i$ response to uniaxial cell stretch in DCM cardiomyocytes.

We explored possible underlying mechanism for the abnormally high stretch responses of TRPV4 and TRPV2 in DCM-hiPSC-CMs. Immunoblot analysis showed no difference in TRPV4 and TRPV2 expression between DCM-hiPSC-CMs and control-hiPSC-CMs (Fig. 4A and Supplementary Fig. 3). Previous studies demonstrated that hypotonicity-induced cell swelling may activate TRPV4 indirectly via a signaling axis involving arachidonic acid-cytochrome P450 epoxygenases-epoxyeicosatrienoic acids [26]. However, in our study, treatment with cytochrome P450 epoxygenase inhibitor MS-PPOH or 17-ODYA failed to alter the stretch-induced $[Ca^{2+}]_i$ response in DCM-hiPSC-CMs (Fig. 4B), suggesting that arachidonic acid and epoxyeicosatrienoic acids were not involved. Another line of ideas is the relationship between cytoskeleton and TRPV4/TRPV2. DCM is often associated with alteration of cytoskeleton arrangement [48]. Previous studies have demonstrated that the mechanical force can act through cytoskeleton to stimulate the activity of TRPV4 and TRPV2 [33,34,49]. Therefore, it is intriguing to propose that an abnormal organization of cytoskeleton in DCM cells could be an underlying reason for the hyperactivity of TRPV4 and TRPV2 under stretch. In agreement, disruption of actin cytoskeleton with cytochalasin D reduced the stretch-induced $[Ca^{2+}]_i$ rise in both cell types, but the effect of cytochalasin D was greater in DCM-hiPSC-CMs than in control-hiPSC-CMs, supporting the notion that the hyperactivity of TRPV4 and TRPV2 may be related to an altered actin cytoskeleton in DCM cardiomyocytes.

5. Conclusions

In conclusion, with the use of patient-specific DCM-ihPSC-CMs as model, we uncovered an abnormally high stretch-induced $[Ca^{2+}]_i$ response in DCM cardiomyocytes, which is related to the activity of TRPV4, and to a lesser degree, TRPV2 and L-type Ca^{2+} channels. It is likely that this abnormal $[Ca^{2+}]_i$ response could be a contributing factor for DCM progression.

Supplementary data to this article can be found online at http://dx.doi.org/10.1016/j.bbadis.2017.07.021.

Transparency document

The Transparency document associated with this article can be found, in online version.

Acknowledgement

This work was supported by grants from the National Science Foundation of China Grant 31470912, Hong Kong Research Grant Committee TBRS/T13-706/11, TBRS/T12-705, AoE/M-05/12, 14118516; National Basic Research Program of China (973 Program, No. 2014CB965102), RGC-NSFC Joint Grant N_CUHK439/13.

References

[1] B.J. Maron, J.A. Towbin, G. Thiene, C. Antzelevitch, D. Corrado, D. Arnett, A.J. Moss, C.E. Seidman, J.B. Young, A. American Heart, H.F. Council on Clinical Cardiology, C. Transplantation, C. Quality of, R. Outcomes, G. Functional, G. Translational Biology Interdisciplinary Working, E. Council on Prevention, Contemporary definitions and classification of the cardiomyopathies: an American Heart Association Scientific Statement from the Council on Clinical Cardiology, Heart Failure and Transplantation Committee; Quality of Care and Outcomes Research and Functional Genomics and Translational Biology Interdisciplinary Working Groups; and Council on Epidemiology and Prevention, Circulation 113 (2006) 1807–1816.
[2] R.E. Hershberger, J.D. Siegfried, Update 2011: clinical and genetic issues in familial dilated cardiomyopathy, J. Am. Coll. Cardiol. 57 (2011) 1641–1649.
[3] W.A. Linke, Sense and stretchability: the role of titin and titin-associated proteins in myocardial stress-sensing and mechanical dysfunction, Cardiovasc. Res. 77 (2008) 637–648.
[4] K.R. Chien, Stress pathways and heart failure, Cell 98 (1999) 555–558.
[5] S. Miyamoto, A.L. Howes, J.W. Adams, G.W. Dorn II, J.H. Brown, Ca^{2+} dysregulation induces mitochondrial depolarization and apoptosis: role of Na^{+}/Ca^{2+} exchanger and AKT, J. Biol. Chem. 280 (2005) 38505–38512.
[6] J.P. Schmitt, M. Kamisago, M. Asahi, G.H. Li, F. Ahmad, U. Mende, E.G. Kranias, D.H. MacLennan, J.G. Seidman, C.E. Seidman, Dilated cardiomyopathy and heart failure caused by a mutation in phospholamban, Science 299 (2003) 1410–1413.
[7] C.K. Du, S. Morimoto, K. Nishii, R. Minakami, M. Ohta, N. Tadano, Q.W. Lu, Y.Y. Wang, D.Y. Zhan, M. Mochizuki, S. Kita, Y. Miwa, F. Takahashi-Yanaga, T. Iwamoto, I. Ohtsuki, T. Sasaguri, Knock-in mouse model of dilated cardiomyopathy caused by troponin mutation, Circ. Res. 101 (2007) 185–194.
[8] K. Haghighi, K.N. Gregory, E.G. Kranias, Sarcoplasmic reticulum Ca-ATPase-phospholamban interactions and dilated cardiomyopathy, Biochem. Biophys. Res. Commun. 322 (2004) 1214–1222.
[9] P. Robinson, P.J. Griffiths, H. Watkins, C.S. Redwood, Dilated and hypertrophic cardiomyopathy mutations in troponin and alpha-tropomyosin have opposing effects on the calcium affinity of cardiac thin filaments, Circ. Res. 101 (2007) 1266–1273.
[10] N. Sun, M. Yazawa, J. Liu, L. Han, V. Sanchez-Freire, O.J. Abilez, E.G. Navarrete, S. Hu, L. Wang, A. Lee, A. Pavlovic, S. Lin, R. Chen, R.J. Hajjar, M.P. Snyder, R.E. Dolmetsch, M.J. Butte, E.A. Ashley, M.T. Longaker, R.C. Robbins, J.C. Wu, Patient-specific induced pluripotent stem cells as a model for familial dilated cardiomyopathy, Sci. Transl. Med. 4 (2012) 130ra147.
[11] S.P. Wyles, X. Li, S.C. Hrstka, S. Reyes, S. Oommen, R. Beraldi, J. Edwards, A. Terzic, T.M. Olson, T.J. Nelson, Modeling structural and functional deficiencies of RBM20 familial dilated cardiomyopathy using human induced pluripotent stem cells, Hum. Mol. Genet. 25 (2016) 254–265.
[12] P.A. Gottlieb, F. Sachs, Cell biology: the sensation of stretch, Nature 483 (2012) 163–164.
[13] J. Teng, S. Loukin, C. Kung, Mechanosensitive ion channels in cardiovascular physiology, Exp. Clin. Cardiol. 20 (2014) 6550–6560.
[14] Y. Iwata, H. Ohtake, O. Suzuki, J. Matsuda, K. Komamura, S. Wakabayashi, Blockade of sarcolemmal TRPV2 accumulation inhibits progression of dilated cardiomyopathy, Cardiovasc. Res. 99 (2013) 760–768.
[15] H.F. Tse, J.C. Ho, S.W. Choi, Y.K. Lee, A.W. Butler, K.M. Ng, C.W. Siu, M.A. Simpson, W.H. Lai, Y.C. Chan, K.W. Au, J. Zhang, K.W. Lay, M.A. Esteban, J.M. Nicholls, A. Colman, P.C. Sham, Patient-specific induced-pluripotent stem cells-derived cardiomyocytes recapitulate the pathogenic phenotypes of dilated cardiomyopathy due to a novel DES mutation identified by whole exome sequencing, Hum. Mol. Genet. 22 (2013) 1395–1403.
[16] L.G. Goldfarb, M.C. Dalakas, Tragedy in a heartbeat: malfunctioning desmin causes skeletal and cardiac muscle disease, J. Clin. Invest. 119 (2009) 1806–1813.
[17] D. Li, T. Tapscoft, O. Gonzalez, P.E. Burch, M.A. Quinones, W.A. Zoghbi, R. Hill, L.L. Bachinski, D.L. Mann, R. Roberts, Desmin mutation responsible for idiopathic dilated cardiomyopathy, Circulation 100 (1999) 461–464.
[18] K. Wahbi, A. Behin, P. Charron, M. Dunand, P. Richard, C. Meune, P. Vicart, P. Laforet, T. Stojkovic, H.M. Becane, T. Kuntzer, D. Duboc, High cardiovascular morbidity and mortality in myofibrillar myopathies due to DES gene mutations: a 10-year longitudinal study, Neuromuscul. Disord. 22 (2012) 211–218.
[19] T. Mochizuki, T. Sokabe, I. Araki, K. Fujishita, K. Shibasaki, K. Uchida, K. Naruse, S. Koizumi, M. Takeda, M. Tominaga, The TRPV4 cation channel mediates stretch-evoked Ca^{2+} influx and ATP release in primary urothelial cell cultures, J. Biol. Chem. 284 (2009) 21257–21264.
[20] H. Mihara, A. Boudaka, T. Sugiyama, Y. Moriyama, M. Tominaga, Transient receptor potential vanilloid 4 (TRPV4)-dependent calcium influx and ATP release in mouse oesophageal keratinocytes, J. Physiol. 589 (2011) 3471–3482.
[21] Y. Qi, Z. Li, C.W. Kong, N.L. Tang, Y. Huang, R.A. Li, X. Yao, Uniaxial cyclic stretch stimulates TRPV4 to induce realignment of human embryonic stem cell-derived cardiomyocytes, J. Mol. Cell. Cardiol. 87 (2015) 65–73.
[22] K. Takahashi, K. Tanabe, M. Ohnuki, M. Narita, T. Ichisaka, K. Tomoda, S. Yamanaka, Induction of pluripotent stem cells from adult human fibroblasts by defined factors, Cell 131 (2007) 861–872.
[23] Y.K. Lee, Y.M. Lau, K.M. Ng, W.H. Lai, S.L. Ho, H.F. Tse, C.W. Siu, P.W. Ho, Efficient attenuation of Friedreich's ataxia (FRDA) cardiomyopathy by modulation of iron homeostasis-human induced pluripotent stem cell (hiPSC) as a drug screening platform for FRDA, Int. J. Cardiol. 203 (2016) 964–971.

[24] H.Y. Kwan, B. Shen, X. Ma, Y.C. Kwok, Y. Huang, Y.B. Man, S. Yu, X. Yao, TRPC1 associates with BK(Ca) channel to form a signal complex in vascular smooth muscle cells, Circ. Res. 104 (2009) 670–678.
[25] J.A. Filosa, X. Yao, G. Rath, TRPV4 and the regulation of vascular tone, J. Cardiovasc. Pharmacol. 61 (2013) 113–119.
[26] H. Watanabe, J. Vriens, J. Prenen, G. Droogmans, T. Voets, B. Nilius, Anandamide and arachidonic acid use epoxyeicosatrienoic acids to activate TRPV4 channels, Nature 424 (2003) 434–438.
[27] S. Kiyonaka, K. Kato, M. Nishida, K. Mio, T. Numaga, Y. Sawaguchi, T. Yoshida, M. Wakamori, E. Mori, T. Numata, M. Ishii, H. Takemoto, A. Ojida, K. Watanabe, A. Uemura, H. Kurose, T. Morii, T. Kobayashi, Y. Sato, C. Sato, I. Hamachi, Y. Mori, Selective and direct inhibition of TRPC3 channels underlies biological activities of a pyrazole compound, Proc. Natl. Acad. Sci. U. S. A. 106 (2009) 5400–5405.
[28] J.M. Richter, M. Schaefer, K. Hill, Clemizole hydrochloride is a novel and potent inhibitor of transient receptor potential channel TRPC5, Mol. Pharmacol. 86 (2014) 514–521.
[29] T. Maier, M. Follmann, G. Hessler, H.W. Kleemann, S. Hachtel, B. Fuchs, N. Weissmann, W. Linz, T. Schmidt, M. Lohn, K. Schroeter, L. Wang, H. Rutten, C. Strubing, Discovery and pharmacological characterization of a novel potent inhibitor of diacylglycerol-sensitive TRPC cation channels, Br. J. Pharmacol. 172 (2015) 3650–3660.
[30] E. Phillips, A. Reeve, S. Bevan, P. McIntyre, Identification of species-specific determinants of the action of the antagonist capsazepine and the agonist PPAHV on TRPV1, J. Biol. Chem. 279 (2004) 17165–17172.
[31] P. Delmas, S.M. Nauli, X. Li, B. Coste, N. Osorio, M. Crest, D.A. Brown, J. Zhou, Gating of the polycystin ion channel signaling complex in neurons and kidney cells, FASEB J. 18 (2004) 740–742.
[32] H. Mihara, N. Suzuki, H. Yamawaki, M. Tominaga, T. Sugiyama, TRPV2 ion channels expressed in inhibitory motor neurons of gastric myenteric plexus contribute to gastric adaptive relaxation and gastric emptying in mice, Am. J. Physiol. Gastrointest. Liver Physiol. 304 (2013) G235–240.
[33] B.D. Matthews, C.K. Thodeti, J.D. Tytell, A. Mammoto, D.R. Overby, D.E. Ingber, Ultra-rapid activation of TRPV4 ion channels by mechanical forces applied to cell surface beta1 integrins, Integr. Biol. (Camb.) 2 (2010) 435–442.
[34] S. Sugio, M. Nagasawa, I. Kojima, Y. Ishizaki, K. Shibasaki, Transient receptor potential vanilloid 2 activation by focal mechanical stimulation requires interaction with the actin cytoskeleton and enhances growth cone motility, FASEB J. 31 (2017) 1368–1381.
[35] S. Ito, B. Suki, H. Kume, Y. Numaguchi, M. Ishii, M. Iwaki, M. Kondo, K. Naruse, Y. Hasegawa, M. Sokabe, Actin cytoskeleton regulates stretch-activated Ca^{2+} influx in human pulmonary microvascular endothelial cells, Am. J. Respir. Cell Mol. Biol. 43 (2010) 26–34.
[36] Z. Wu, K. Wong, M. Glogauer, R.P. Ellen, C.A. McCulloch, Regulation of stretch-activated intracellular calcium transients by actin filaments, Biochem. Biophys. Res. Commun. 261 (1999) 419–425.
[37] J.F. Casella, M.D. Flanagan, S. Lin, Cytochalasin D inhibits actin polymerization and induces depolymerization of actin filaments formed during platelet shape change, Nature 293 (1981) 302–305.
[38] S. Chandar, L.S. Yeo, C. Leimena, J.C. Tan, X.H. Xiao, V. Nikolova-Krstevski, Y. Yasuoka, M. Gardiner-Garden, J. Wu, S. Kesteven, L. Karlsdotter, S. Natarajan, A. Carlton, S. Rainer, M.P. Feneley, D. Fatkin, Effects of mechanical stress and carvedilol in lamin A/C-deficient dilated cardiomyopathy, Circ. Res. 106 (2010) 573–582.
[39] V. Nikolova, C. Leimena, A.C. McMahon, J.C. Tan, S. Chandar, D. Jogia, S.H. Kesteven, J. Michalicek, R. Otway, F. Verheyen, S. Rainer, C.L. Stewart, D. Martin, M.P. Feneley, D. Fatkin, Defects in nuclear structure and function promote dilated cardiomyopathy in lamin A/C-deficient mice, J. Clin. Invest. 113 (2004) 357–369.
[40] C.L. Hooper, A. Paudyal, P.R. Dash, S.Y. Boateng, Modulation of stretch-induced myocyte remodeling and gene expression by nitric oxide: a novel role for lipoma preferred partner in myofibrillogenesis, Am. J. Physiol. Heart Circ. Physiol. 304 (2013) H1302–1313.
[41] K.G. Shyu, Cellular and molecular effects of mechanical stretch on vascular cells and cardiac myocytes, Clin. Sci. 116 (2009) 377–389.
[42] H. Toko, H. Takahashi, Y. Kayama, T. Oka, T. Minamino, S. Okada, S. Morimoto, D.Y. Zhan, F. Terasaki, M.E. Anderson, M. Inoue, A. Yao, R. Nagai, Y. Kitaura, T. Sasaguri, I. Komuro, Ca^{2+}/calmodulin-dependent kinase IIdelta causes heart failure by accumulation of p53 in dilated cardiomyopathy, Circulation 122 (2010) 891–899.
[43] A. Belus, E. White, Streptomycin and intracellular calcium modulate the response of single guinea-pig ventricular myocytes to axial stretch, J. Physiol. 546 (2003) 501–509.
[44] K. Hongo, E. White, J.Y. Le Guennec, C.H. Orchard, Changes in $[Ca^{2+}]_i$, $[Na^+]_i$ and Ca^{2+} current in isolated rat ventricular myocytes following an increase in cell length, J. Physiol. 491 (Pt 3) (1996) 609–619.
[45] A. Kamkin, I. Kiseleva, G. Isenberg, Ion selectivity of stretch-activated cation currents in mouse ventricular myocytes, Pflugers Arch. 446 (2003) 220–231.
[46] J. Soboloff, M. Spassova, W. Xu, L.P. He, N. Cuesta, D.L. Gill, Role of endogenous TRPC6 channels in Ca^{2+} signal generation in A7r5 smooth muscle cells, J. Biol. Chem. 280 (2005) 39786–39794.
[47] D.M. Bers, Cardiac excitation-contraction coupling, Nature 415 (2002) 198–205.
[48] V. Sequeira, L.L. Nijenkamp, J.A. Regan, J. van der Velden, The physiological role of cardiac cytoskeleton and its alterations in heart failure, Biochim. Biophys. Acta 1838 (2014) 700–722.
[49] C. Goswami, J. Kuhn, P.A. Heppenstall, T. Hucho, Importance of non-selective cation channel TRPV4 interaction with cytoskeleton and their reciprocal regulations in cultured cells, PLoS One 5 (2010) e11654.